

A Testbed for Studying Automatic Dependent Surveillance Broadcast (ADS-B) Based Range and Positioning Performance to Support Alternative Position Navigation and Timing (APNT)

Yu-Hsuan Chen, *Stanford University*
Sherman Lo, *Stanford University*

Dennis M. Akos, *University of Colorado at Boulder*
Gabriel Wong, *Stanford University*
Per Enge, *Stanford University*

BIOGRAPHY

Yu-Hsuan Chen is a postdoctoral scholar at the Stanford GPS Laboratory. He received his Ph.D. in electrical engineering from National Cheng Kung University, Taiwan. His research interests include real-time GNSS software receiver, antenna array processing and APNT.

Sherman Lo is currently a senior research engineer at the Stanford GPS Laboratory. He is the Associate Investigator for the Stanford University efforts on the FAA evaluation of alternative position navigation and timing (APNT) systems for aviation. He received the Ph.D. in Aeronautics and Astronautics from Stanford University.

Dennis M. Akos obtained the Ph.D. degree from Ohio University in 1997. He is an associate professor with the Aerospace Engineering Science Department at University of Colorado at Boulder with visiting appointments at Luleå Technical University and Stanford University.

Gabriel Wong is an Electrical Engineering Ph.D. candidate at the Stanford GPS Laboratory under the guidance of Professor Per Enge. He has previously received an M.S.(EE) from Stanford University, and a B.S.(EECS) from UC Berkeley. His current research involves signal deformation monitoring and mitigation for GNSS signals.

Per Enge is a professor of Aeronautics and Astronautics at Stanford University, where he is the Vance D. and Arlene C. Coffman Professor in the School of Engineering. He directs the Stanford GPS Laboratory, which develops satellite navigation systems. He has been involved in the development of the Federal Aviation Administration's GPS Wide Area Augmentation System (WAAS) and Local Area Augmentation System (LAAS).

ABSTRACT

As air traffic continues to grow, the Global Navigation Satellite System (GNSS) plays an increasingly important role in enabling the air space to efficiently handle the increase load. In fact, it will be the primary and often the only system capable of supporting key capabilities for the future airspace. However, GNSS is vulnerable to radio frequency interference (RFI) and spoofing, so an alternative position, navigation and timing (APNT) system that also enables many of GNSS derived capabilities is necessary for aviation user.

While APNT can be developed in many ways, the use of existing signals is preferred as new signals would require new equipment, spectrum allocation and incur a host of other complex institutional challenges. Automatic Dependent Surveillance Broadcast (ADS-B) and related signals such as Traffic Information Surveillance Broadcast (TIS-B) is an attractive candidate to provide an APNT signal. It is a major surveillance technology being adopted by aircraft and air navigation service providers worldwide. In ADS-B, an aircraft broadcasts its precise

position derived currently from GNSS. Additionally, ADS-B and TIS-B signals could be used for multilateration or passive ranging to provide APNT, potentially with little modification.

We built a testbed to assess ranging performance and calculate position solution using ADS-B and TIS-B signals on the international Mode S Extended Squitter (ES) standard. The test equipment was developed using relative low cost components and was setup at multiple sites. The geographically separated sites are synchronized by GPS and Rubidium clock. We conduct three tests: time synchronization, ranging assessment and positioning solution. The testing results show that the ranging and positioning performance could meet targeted APNT accuracy levels.

INTRODUCTION

The Federal Aviation Administration (FAA) Alternative Position Navigation and Timing (APNT) effort seeks to develop navigation service to continue efficient, high-density operations even if Global Navigation Satellite System (GNSS) service is degraded. One technology being examined to support APNT is Automatic Dependent Surveillance Broadcast (ADS-B). ADS-B is being currently implemented to provide improved surveillance capabilities. An ADS-B equipped aircraft broadcasts its precise positions derived from GNSS to provide high accuracy surveillance for air traffic control and traffic awareness to nearby aircraft. Additionally, ADS-B ground stations, sometimes called ground based transceivers (GBT), re-transmit ADS information, known as ADS-R (R for rebroadcast), as well as provide traffic information service-broadcast (TIS-B). Mode S Extended Squitter (ES), transmitted on 1090 MHz, is the most commonly used ADS-B signal and it is an internationally adopted standard. Other signals are also being developed for ADS-B. This work investigates the performance of Mode S ES ADS-B signals to provide APNT capabilities.

ADS-B and APNT are complementary technologies. APNT can provide the accurate navigation information needed by ADS-B. Currently ADS-B relies on GNSS for its position reports. Hence APNT improves ADS-B availability and robustness. The ADS-B system offers multiple possible means to provide an APNT capability. One means is to use ADS-B and its related signals to provide passive or “pseudo” ranging [1]. In the United

States, the ADS-B transmission uses either 1090 MHz Mode S ES or 978 MHz Universal Access Transceiver (UAT). UAT has passive ranging (PR) features built into its transmissions from an ADS-B ground station. We have been studying how to modify Mode S ES to provide PR with a minimal amount of changes. Another possibility is to use the ground based multilateration (MLAT) that is being developed and implemented to provide verification of ADS-B data. MLAT derived position, when transmitted from the ground back to the aircraft, may serve as a source of navigation information. Hence, two major aspects of our APNT effort examine the ranging capabilities of the ADS-B signals and the positioning performance with ADS-B based MLAT.

The work in this paper focuses on the 1090 MHz signal. A multi-signal testbed was developed using relatively low cost commercial off the shelf (COTS) components. The main components are data collection systems built using the universal software receiver peripheral (USRP) which collects raw 1090 signals. As MLAT or PR requires multiple geographically separated but synchronized measurements of the same signal, a means of synchronizing the data from each data collection unit was developed. The developed method also synchronizes each of the measured ADS-B signal sample with a GPS sample at each given data collection unit or site. This allows for synchronization of the samples between geographically separated data collection units and for calculation of position.

We conduct three different tests with the testbed. The first test examines the time synchronization performance of our equipment. The second test performs a two-site time difference of arrival (TDOA) test to assess the ranging capability of 1090 Mode S ES signal. The third test used measurements from three sites demonstrating the performance of 1090 Mode S ES when conducting PR or MLAT based positioning.

This paper is organized as follows. First, 1090 signals are introduced. Then, an overview of MLAT and PR is given. We then explain how the ranging measurements of 1090 signals are obtained. The development of equipment and testbed are then described. Finally, the test setups and results for each test are detailed.

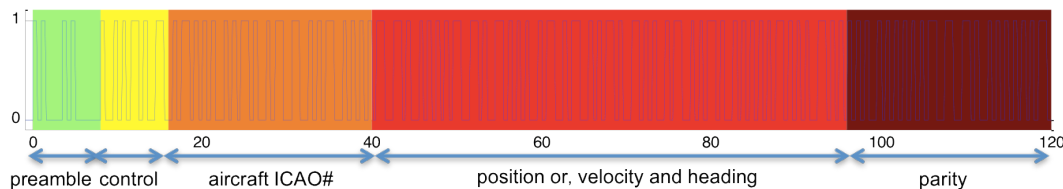


Figure 1. Example of an ADS-B message

INTRODUCTION OF 1090 SIGNALS

1090 MHz has long been dedicated by aviation for surveillance and identification dating back to its use for identifying friend or foe (IFF). There are several modes or transmission types on 1090 MHz with the most important ones being mode A/C/S for civil and mode 1/2/3 for military aviation. The original Mode S signal provides the surveillance such as air-to-air, altitude and identification reply. Mode S Extended Squitter (ES) provides increased data capacity (88 bits) which allows for its use for Automatic Dependent Surveillance-Broadcast (ADS-B).

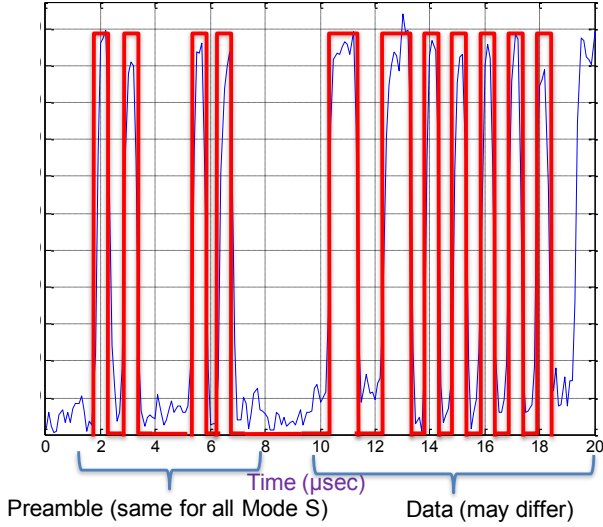


Figure 2. Mode S and Mode S ES preamble pulses: captured (blue) and ideal (red)

An example of ADS-B message is depicted in figure 1 [2]. It includes the preamble which indicates the mode. Mode S is indicated by having four 0.5 microseconds (μsec) pulses with the last three coming 1, 2.5 and 3.5 μsec after the first. This is seen in detail in figure 2. The 88-bit message field includes the aircraft's International Civil Aviation Organization (ICAO) number and can include aircraft's position or, velocity and heading. ADS-B ground stations transmit the Traffic Information Services-Broadcasts (TIS-B) on 1090 MHz Mode S ES. This broadcast is structurally the same as 1090 ADS-B, including the same preamble as both are Mode S transmissions. TIS-B is indicated in the message data by a different downlink format (DF). This service allows non-ADS-B equipped aircrafts to be tracked by ADS-B equipped aircrafts by having the GBT broadcast the locations of non-ADS-B equipped as derived by ground radar. We also use the TIS-B signal for evaluating ranging. Other 1090 MHz modes are not as useful for APNT and hence represent interference to the desired Mode S signals.

MULTILATERATION AND PASSIVE RANGING

Two potential approaches to provide APNT are PR and MLAT in the same manner as GNSS. In PR, the aircraft receives multiple signals (ADS-B IN) from ground stations and then calculates its position. MLAT starts from aircraft broadcasting an ADS-B signal (ADS-B OUT). The ranging measurements are made by ground stations receiving the ADS-B signal. If at least three ground stations receive the same signal, then the aircraft's position can be calculated – typically at a central server. As seen in figure 3 [3], PR and MLAT make essentially the same measurements. The difference is where the position calculated is made. One requirement for both approaches is time synchronization between ground stations because ranging measurement depends on traveling time of signals.

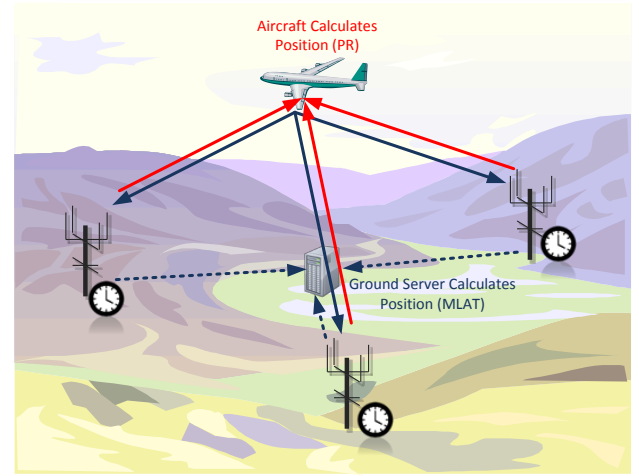


Figure 3. Architecture of multilateration (MLAT) and passive ranging (PR)

OBTAINING RANGING MEASUREMENT

The lack of timing information in 1090 ADS-B message (see figure 1) necessitates differential measurements to assess ranging performance. One method is to use time difference of arrival (TDOA) made by differencing time of arrival (TOA) from two geographically separated stations. Equation 1 shows this where TOA_k is the TOA measured by the k^{th} site. TDOA represents an estimate of the differential travel time from the 1090 source to two ground stations as shown in figure 4.

$$TDOA = (TOA_1 - TOA_2) \quad (1)$$

The dotted lines represent the travel distance of signal estimated from TOA. This measurement includes errors from signal in space (SIS) and clock synchronization. Additionally, one needs the time of transmission (TOT), which is not known. The TDOA calculation is used since TOT cancels out when calculating TDOA. TDOA times the speed of signal propagation, c , yields the estimate

differential distance. The true differential distance is calculated from true distance between source and two reference stations (data collection sites) in equation (2).

$$\Delta d = d_1 - d_2 \quad (2)$$

The distances d_1, d_2 are calculated with the known surveyed positions of the two stations and aircraft's reported position from 1090 ADS-B message. Even though this is our reference or truth measure, the aircraft reported position has several error sources. Due to bandwidth limitations on 1090 Mode S ES, the broadcast has limited resolution. The position accuracy of compact positioning report (CPR) used in the message for encoding latitude and longitude is 5.1 m [2]. Another error comes from extrapolating the moving aircraft position to a future time. If the extrapolation flag set, the position is extrapolated to exact 0.2 second epoch and loaded between 50 ~ 150 milliseconds before that epoch. As the broadcast is typically not sent at the exact 0.2 second interval, there are both errors from the extrapolation and from transmitting at a different time than the time of the extrapolated position. Finally, the broadcast altitude also has a quantization error of 25 feet. If TIS-B is used, the source is the ground station and its location is gathered from a database and verified by maps.

Range error (RE) is determined by calculating the error between the TDOA estimated differential distance and the true differential distance. This is seen in Equation 3.

$$RE = c * TDOA - \Delta d \quad (3)$$

RE will be used to assess the ranging performance in the following sections.

Time synchronization between stations is the key to accurate TDOA estimates. GPS is used to get time stamp for all samples taken at each station. A Rubidium ovenized crystal oscillator (RbOCXO) sets the sampling clock so that the drift between samples is minimized. As discussed later, it is also used to synchronize sampling between the 1090 MHz and GPS components of the data collection unit. This system also emulates a potential APNT time synchronization concept.

Operationally, GNSS may be used for synchronization. APNT has been developing Controlled Reception Pattern Antenna (CRPA) array for using GNSS for precise time synchronization [4-7]. This increases jamming resistance by more than 30 dB against various forms of interference. A high quality oscillator such as a RbOCXO would be part of the time synchronization system. The characteristic of clock such as bias and drift can be estimated during interference-free periods. Once the station is attacked by strong interference and loses GNSS reception, the internal oscillator adequate synchronization for extended periods.

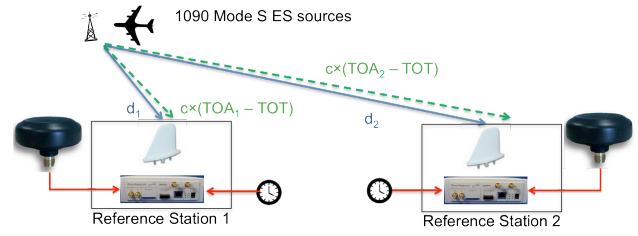


Figure 4. TDOA ranging measurement

DEVELOPMENT OF TEST EQUIPMENT

Based on the requirement for measuring TDOA, we developed test equipment capable of receiving and collecting 1090 and GPS signals aligned by sampling time. The hardware architecture of test equipment is depicted in figure 5. The hardware contains one GPS antenna, one 1090 antenna, one tunable filter for 1090, one RBOCXO, two USRPs [8], one for each signal, and one host computer. The received GPS and 1090 signals pass to USRPs, which are equipped with a DBSRX2 programmable mixing and down-conversion daughter boards. A 10 MHz external signal from a common Rubidium clock synchronizes the data collection from both USRPs. The USRPs are controlled by a host computer running the Ubuntu distribution of Linux. The USRP hardware driver (UHD) [9] software is used to configure USRP2 and daughter boards settings such as sampling rate and RF center frequency. This flexible hardware set up supports a synchronized two-antenna signal collection system and real-time software receiver [10,11]. The radio frequency (RF) signal from each antenna element is converted to a near zero Intermediate Frequency (IF) and digitized to 14-bit complex or in-phase and quadrature outputs (I & Q, respectively). The RF center frequency is set to 1575 MHz for GPS and 1090 MHz for 1090. The sampling rate is set to 10 Megasamples per second (MSPS). The digitalized IF data is then processed in real-time and/or stored into hard drive in the host computer. Figure 6 shows a picture of the test equipment.

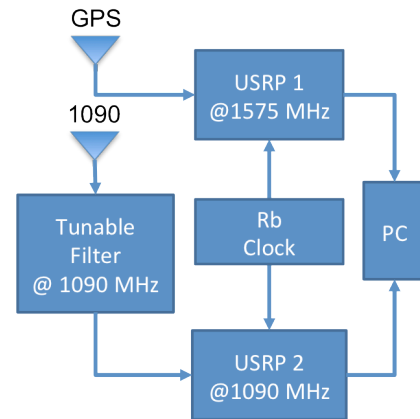


Figure 5. Block diagram of test equipment

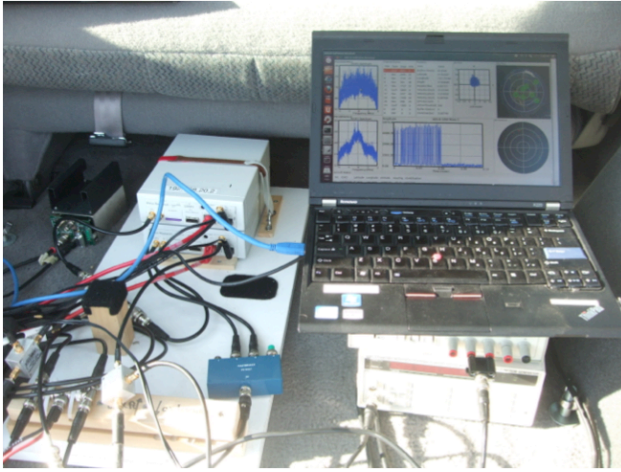


Figure 6. Data Collection Test Equipment Set up

1090 ASSESSMENT TESTBED

In order to assess the 1090 signal for ranging and positioning, we built several data collection units and tested them as illustrated in figure 7. Three ground sites on Stanford campus were set up with the data collection units previously discussed. The sources of 1090 signal come from aircraft or ADS-B ground stations.

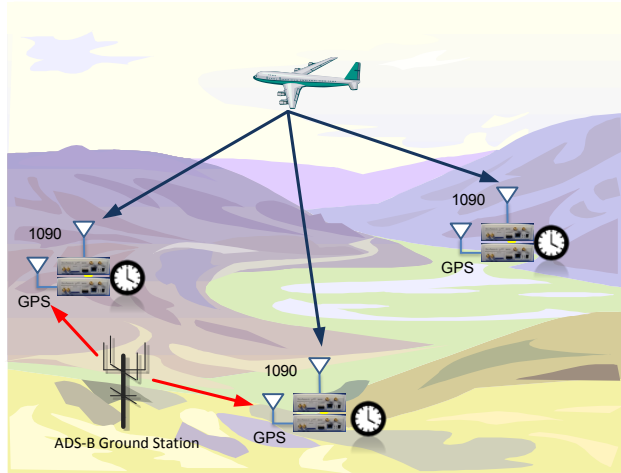


Figure 7. 1090 assessment testbed

Table 1. Tests in 1090 testbed

Tests	1090 signal sources	Sites number
zero baseline	aircraft	1
Ranging assessment	aircraft or ground station	2
Positioning solution	aircraft	3

ZERO BASELINE TEST

The time synchronization performance of our equipment is evaluated by a zero baseline test. The set up is seen in figure 8 with two data collection units capturing signals from the same 1090 and GPS antennas. As the distance between the signal sources for the data collection units is zero, the ideal TDOA should be zero. However, there will still be errors due to our ability to measure the signal as well as other sources from equipment, differential line delays and signal strength. Additionally, there is our sampling resolution – samples are taken every 100 ns. Processing was developed to handle the sampling resolution error. Figure 9 shows the TDOA over time and figure 10 shows the corresponding histogram. The standard deviation of zero-baseline TDOA is about 8.78 ns or 2.63 m. The results are reasonable for our test needs and are adequate for evaluating whether the range accuracy can meet APNT targets. Also, the time synchronization meets APNT targeted accuracy of less than 50 ns [12].

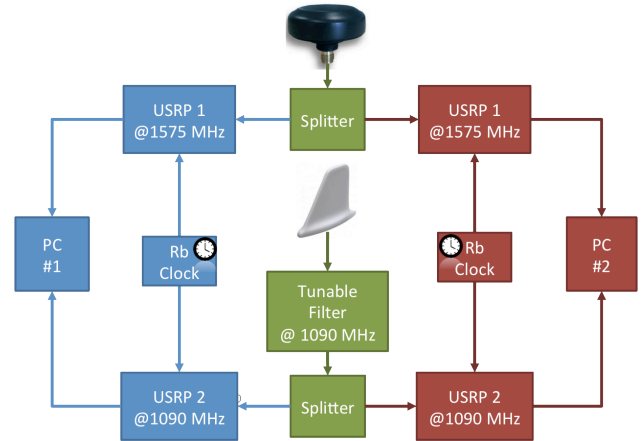


Figure 8. Zero baseline test setup for time synchronization

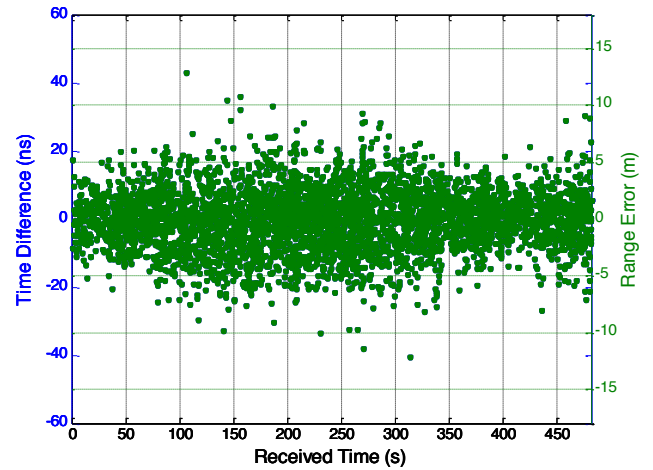


Figure 9. TDOA vs. time in the zero baseline test

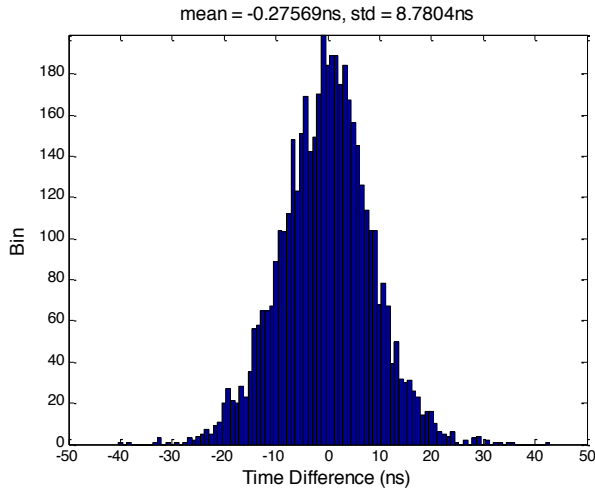


Figure 10. Histogram of TDOA in the zero baseline test

RANGING ASSESSMENT TEST

We set up the data collection units at two elevated sites separated by 663 meters, as seen in figure 11. Both ADS-B signals from moving aircrafts or TIS-B signal from static ground station are collected. ADS-B signals from moving aircrafts experience more diverse environmental effects. Thus, signal in space (SIS) errors such as multipath are worse. Figure 12 shows ADS-B TDOA range error over time and figure 13 shows the corresponding error histogram. The resulting range error has a mean of 7.7 m and a standard deviation of 15 m. The 7-sigma lines are shown in the histogram. The percentage of occurrence outside these lines should be less than 3×10^{-12} . However, four outliers were found and required investigation. The waveforms of both sites are depicted in figure 14. The blue and green curves show the amplitude of preamble pulses collected from site 1 and 2. Compare the preamble with that shown in figure 2. One can see that there is some distortion or adulteration in one of the two preambles of each outlier case resulting in TOA errors. In the figure 14, the solid vertical line represents the TOA calculated by our developed software. The dotted vertical line represents the expected TOA derived from the locations of the source aircraft and ground stations and assuming the stronger TOA is correct. When we look into four waveforms, all outliers have one clear signal from one site and an adulterated signal from the other site. By analyzing the shape and amplitude of waveform, we can hypothesize the potential cause of the outliers as seen in table 2. Generally, the error is caused by multipath and in some cases we can identify the source of reflection. One case is caused by having a weak signal at one site.



Figure 11. Site arrangement for ranging assessment test

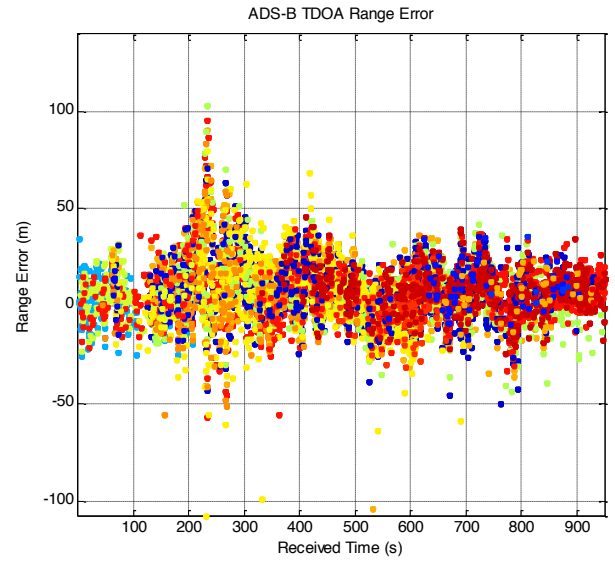


Figure 12. ADS-B TDOA range error in the ranging assessment test

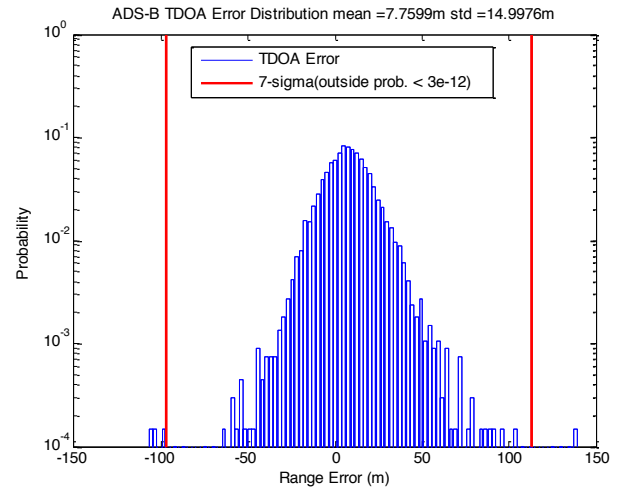


Figure 13. ADS-B TDOA range error histogram in the ranging assessment test

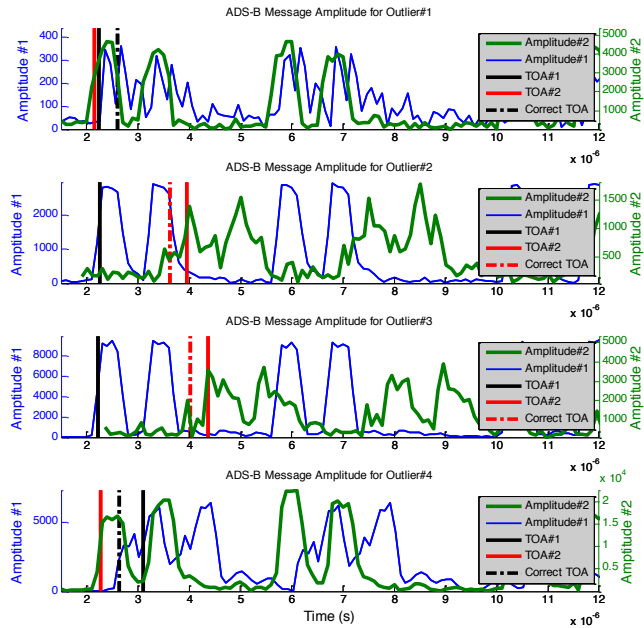


Figure 14. ADS-B message waveforms of outliers in the ranging assessment test (4 outlier cases shown)

Table 2. Potential cause of outliers in ranging assessment test

Outlier	Adulterated signal	Potential Cause
1	1	Weak signal
2	2	multipath
3	2	multipath
4	1	multipath

TIS-B signal from an ADS-B ground station do not have motion-induced errors. Hence any errors in its location should show up as a bias. The TIS-B collection from the San Carlos/Woodside ADS-B ground station is shown in figure 15. TDOA range performance from this TIS-B source over time and its corresponding histogram is shown in figure 16 and figure 17, respectively. As expected, the resulting range error is better than that from aircraft sources with a mean of 4.3 m and a standard deviation of 11.6 m. Also, there are no outliers outside the 7-sigma lines.



Figure 15. Ground station location and its distance to two sites

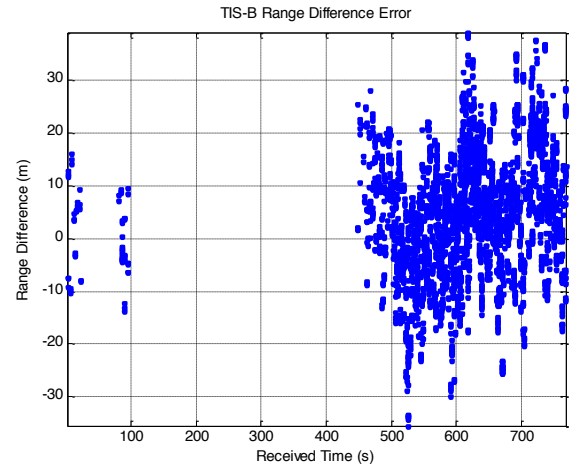


Figure 16. TIS-B TDOA range error in the ranging assessment test

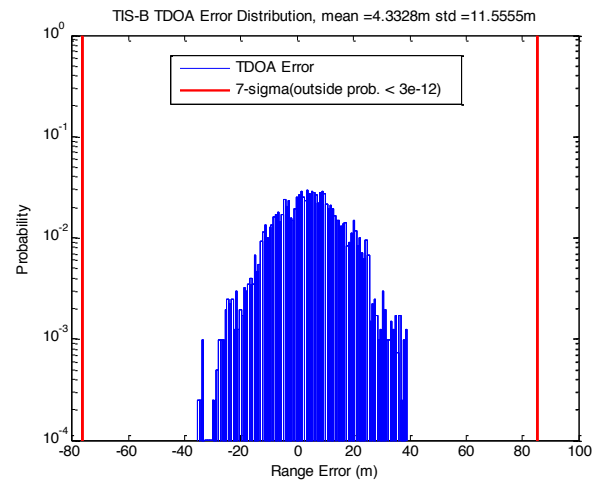


Figure 17. TIS-B TDOA range error histogram in the ranging assessment test

POSITIONING SOLUTION TEST

For the positioning test, we set up three sites as shown in figure 18. Following equations are used to solve the aircraft's position.

$$\begin{aligned} c \times (TOA_1 - TOA_2) &= \sqrt{(x-x_1)^2 + (y-y_1)^2 + (z-z_1)^2} - \sqrt{(x-x_2)^2 + (y-y_2)^2 + (z-z_2)^2} \\ c \times (TOA_1 - TOA_3) &= \sqrt{(x-x_1)^2 + (y-y_1)^2 + (z-z_1)^2} - \sqrt{(x-x_3)^2 + (y-y_3)^2 + (z-z_3)^2} \\ h &= F(x, y, z) \end{aligned} \quad (4)$$

where c is speed of light, TOA_k is the time of arrival of k^{th} site, x, y, z is the aircraft's position to be solved, x_k, y_k, z_k is the surveyed position of k^{th} site, h is barometric altitude which is obtained from ADS-B messages, and F is the function to transfer earth-centered earth-fixed (ECEF) Cartesian coordinate frame (x, y, z) to the h in ellipsoidal coordinate [13]. Figure 19 shows the processing flow in calculating position. It starts from obtaining TOA from all sites and aircraft's altitude from ADS-B message. As only horizontal position is to be solved, the altitude is fixed. The aircraft position is then solved with the known positions of sites using an iterative least squared method.

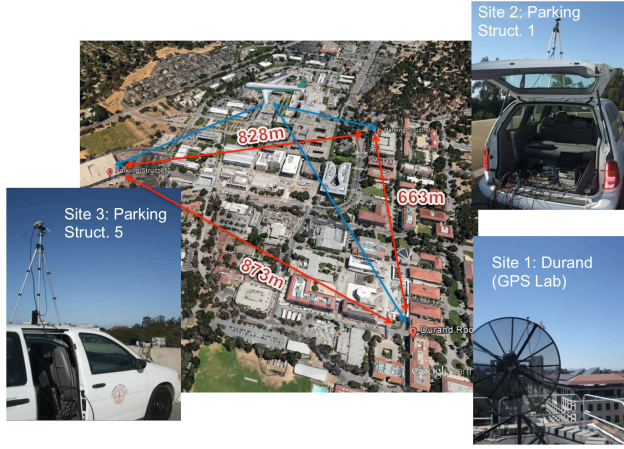


Figure 18. Site arrangement for positioning solution test

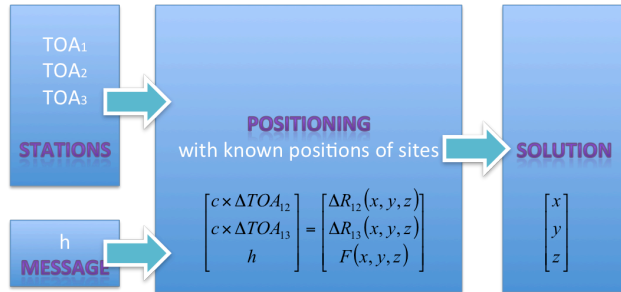


Figure 19. Positioning procedure

Figure 20 shows the positioning result. The three triangles indicate the locations of three data collection sites. The curves with different color represent the positions from different aircraft, which are decoded from their ADS-B

messages. The black dots are the calculated position solutions. Only positions close to three sites could be calculated as geometry of sites limits the range with which our processing yields a solution. Figure 21 and figure 22 show the positioning error along with the position dilution of precision (PDOP) and altitude for two aircrafts. From these figures, we notice that the positioning error highly depends on PDOP. Aircraft that are far from the sites have very high PDOPs which prevents the solution from converging. Figure 23 shows the equivalent range error (ERE), which is calculated by dividing the positioning error by PDOP. Its mean value is 15.75 m, which is similar to our calculated range performance.

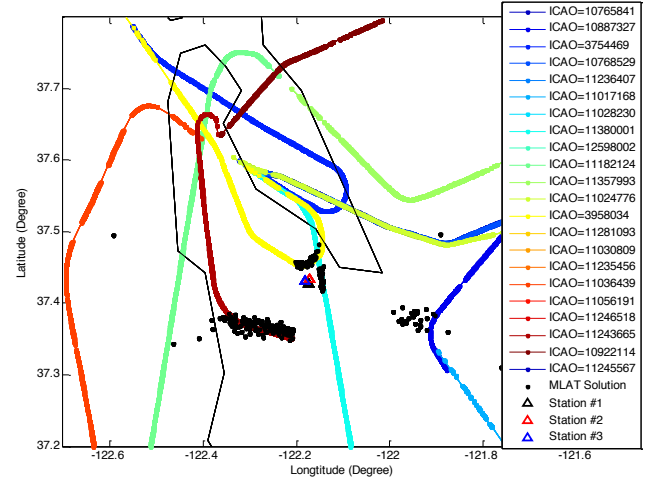


Figure 20. Positioning results in the positioning solution test

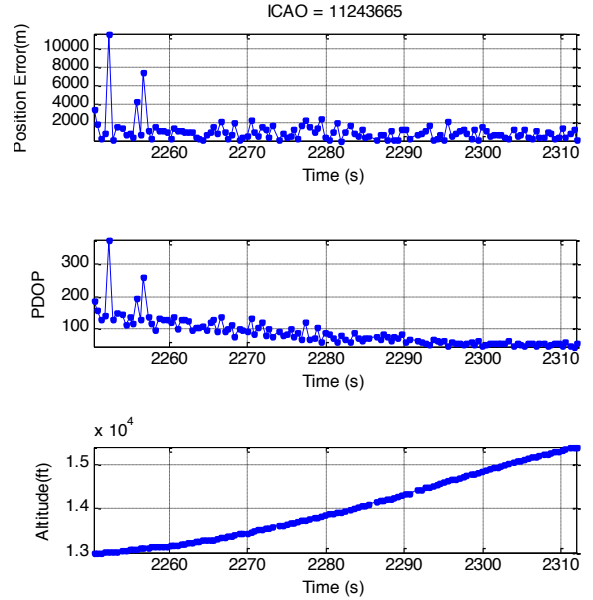


Figure 21. Example I: Position error, PDOP and aircraft's altitude

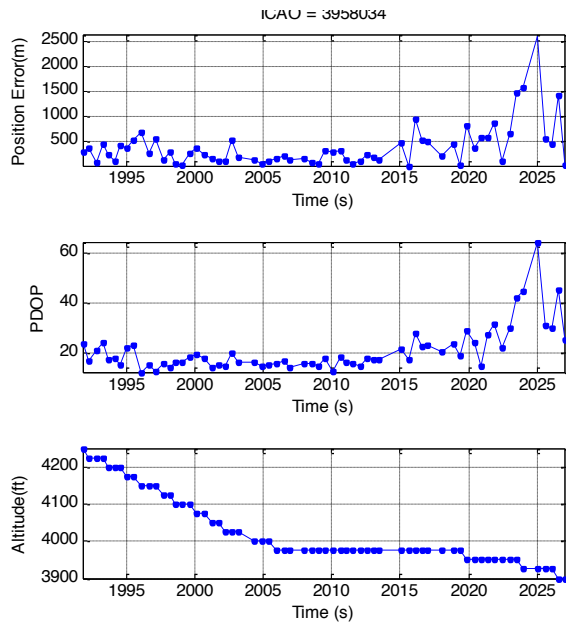


Figure 22. Example II: Position error, PDOP and aircraft's altitude

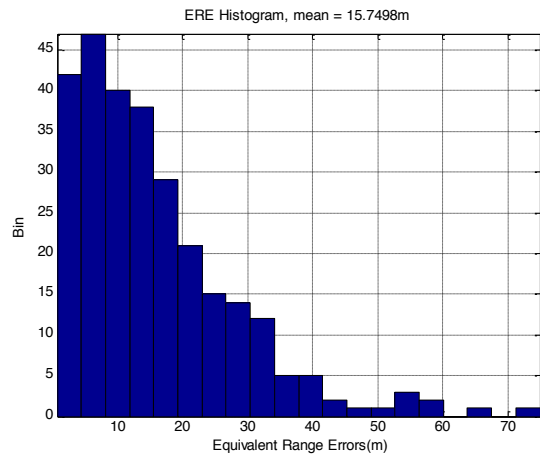


Figure 23. ERE result in the positioning solution test

CONCLUSIONS

Our tests demonstrated the feasibility and capability of using 1090 ADS-B signals for positioning – whether by passive ranging or multilateration. The first test demonstrated that we can achieve highly precise time synchronization with a standard deviation of 2.63m. Our range evaluation showed that ADS-B TDOA differential range error can be adequate for APNT. The results show a standard deviation of 15 m for most aircraft within range. The actual performance may be a little different as this assumes that the aircraft broadcast position has no error which is not true. However, it is likely that if the aircraft broadcast position errors were eliminated, the range performance would be better. Indeed, the ADS-B (aircraft derived) TDOA range error estimate is likely conservative as TIS-B TDOA range error has a lower standard

deviation (11.5 m). These results suggest that the 1090 Mode S ES signal has good potential to support ranging even the most stringent APNT ranging targets (100 m or 27 m with a worst case horizontal dilution of precision of 2.8) [1].

This work also demonstrated positioning using 1090 Mode S ES signals. The positioning assessment showed a mean ERE of 15.75m. Given this ERE performance, 1090 has good potential for meeting the APNT target accuracy (100 m), particularly if the geometry of ground stations or PDOP has a value less than 6.

ACKNOWLEDGMENTS

The authors gratefully acknowledge the FAA CRDA 12-G-003 for supporting this research. They also acknowledge the FAA APNT team for their support and insights.

REFERENCES

- [1] S. Lo, "Pseudolite Alternatives for Alternate Positioning, Navigation, and Timing (APNT)," FAA White Paper, August 2012, reachable on the web at http://www.faa.gov/about/office_org/headquarters_offices/ato/service_units/techops/navservices/gnss/library/documents/APNT/media/APNT_Pseudolite_WhitePaper_Final.pdf
- [2] RTCA DO-260A, Minimum operational performance standards for 1090 MHz Extended Squitter Automatic Dependent Surveillance-Broadcast (ADS-B) and Traffic Information Services-Broadcast (TIS-B), 2003.4.10.
- [3] F. A. Niles, R. S. Conker, M. B. El-Arini, D. G. O'Laughlin, D. V. Baraban, "Wide Area Multilateration for Alternate Position, Navigation, and Timing (APNT)," White Paper, August 2012, reachable on the web at http://www.faa.gov/about/office_org/headquarters_offices/ato/service_units/techops/navservices/gnss/library/documents/APNT/media/WAM_WhitePaperFINAL_MITRE_v2.pdf
- [4] Y.-H. Chen, D. S. De Lorenzo, J. Seo, S. Lo, J.-C. Juang, P. Enge, and D. M. Akos, Real-Time Software Receiver for GPS Controlled Reception Pattern Array Processing," Proceedings of ION GNSS 2010, Portland, OR, September 2010, pp. 1932-1941.
- [5] Y.-H. Chen, J.-C. Juang, J. Seo, S. Lo, D.M. Akos, D. S. De Lorenzo, P Enge, "Design and Implementation of Real-Time Software Radio for Anti-Interference GPS/WAAS Sensors," Sensors 2012, 12, pp. 13417-13440.

[6] Y.-H. Chen, "A Study of Geometry and Commercial Off-The-Shelf (COTS) Antennas for Controlled Reception Pattern Antenna (CRPA) Arrays," Proceedings of ION GNSS 2012, Nashville, TN, September 2012, pp. 907-914.

[7] Y.-H. Chen, S. Lo, D.M. Akos, D. S. De Lorenzo, P. Enge, "Validation of a Controlled Reception Pattern Antenna (CRPA) Receiver Built From Inexpensive General-purpose Elements During Several Live-jamming Test Campaigns," Proceedings of ION ITM 2013, San Diego, California, January 2013, pp. 154-163.

[8] USRP2 motherboard and DBSRX2 programmable daughterboard, Ettus Research LLC, reachable on the web at <http://www.ettus.com>.

[9] UHD - USRP Hardware Driver, Ettus Research LLC, reachable on the web at http://files.ettus.com/uhd_docs/manual/html/.

[10] U.S. Patent No. 7,305,021, "Real-Time Software Receiver," Awarded Dec. 4, 2007, by B.M. Ledvina, M.L. Psiaki, S.P. Powell, and P.M. Kintner, Jr.

[11] Y.-H. Chen and J.-C. Juang, "A GNSS Software Receiver Approach for the Processing of Intermittent Data," Proceedings of ION GNSS 2007, Fort Worth, TX, September 2007, pp. 2772-2777.

[12] M. Narins, P. Enge, B. Peterson, S. Lo, Y.-H. Chen, D. Akos, M. Lombardi, "The Need for a Robust Precise Time and Frequency Alternative to Global Navigation Satellite Systems," Proceedings of ION GNSS 2012, Nashville, TN, September 2012, pp. 2057-2062.

[13] P. Misra and P. Enge, Global Positioning System: Signals, Measurement, and Performance, 2nd Edition, Ganga-Jamuna Press, Lincoln, MA. , 2006